Hindawi
Shock and Vibration
Volume 2020, Article ID 8180612, 14 pages
https://doi.org/10.1155/2020/8180612

Research Article

Comparison of Scaling Ground Motions Using Arithmetic with Logarithm Values for Spectral Matching Procedure

Rui Zhang[1,2], **Dong-sheng Wang**[1,3], **Xiao-yu Chen**[4] and **Hong-nan Li**[1]

[1]*State Key Laboratory of Coastal and Offshore Engineering, Dalian University of Technology, Dalian 116024, China*
[2]*School of Civil Engineering, Dalian Jiaotong University, Dalian 116028, China*
[3]*School of Civil and Transportation Engineering, Hebei University of Technology, Tianjin 300401, China*
[4]*Institute of Road and Bridge Engineering, Dalian Maritime University, Dalian 116026, China*

Correspondence should be addressed to Dong-sheng Wang; dswang@hebut.edu.cn

Received 7 August 2019; Accepted 10 December 2019; Published 3 January 2020

Academic Editor: Nuno M. Maia

In recent studies, spectral matching is the most commonly proposed method for selecting earthquake records for time-history analysis of structures. However, until now, there have been no serious investigations of the effects of coordinate values on the scaling of ground motions. This paper investigated the influence of using arithmetic and logarithmic values of response spectra in spectral matching procedures (i.e., ASM and LSM methods) on the results of nonlinear structural time-history analysis. Steel moment resisting frame structures of the 3-, 9-, and 20-stories, which represent low-, medium-, and high-rise buildings, respectively, were used as examples. Structural benchmark responses were determined by calculating the arithmetic mean and median of peak interstory drift ratio (PIDR) demands based on the three record sets developed by the American SAC Steel Project. The three record sets represent seismic hazard levels with 50%, 10%, and 2% probabilities exceeded in 50 years, and their average acceleration spectra were also taken as the target spectrum. Moreover, another 40 record components for selection were scaled both by ASM and LSM methods. The seven components whose spectra were best compatible with the target spectra were selected for the structural time-history analysis. The scale factors obtained by the LSM method are nearly larger than that of the ASM method, and their ranking and selection of records are different. The estimation accuracies of structural mean (median) responses by both methods can be controlled within an engineering acceptable range (±20%), but the LSM method may cause larger structural responses than the ASM method. The LSM method has a better capacity for reducing the variability of structural responses than the ASM method, and this advantage is more significant for longer-period structures (e.g., 20-story structure) with more severe nonlinear responses.

1. Introduction

The nonlinear time-history analysis has been a widely accepted method for seismic design and assessment of structures, also being the most prevalent process used for performance-based design [1–4]. According to the seismic design codes (e.g., Eurocode 8 [5] and ASCE 7-16 [6]), time-history analyses are typically conducted with 7 or 11 ground motions records, and the arithmetic mean of the engineering demands parameters (EDPs) (e.g., story drifts and rotation capacity of plastic hinge) are taken as the reference results for the design [2, 7, 8]. However, the results of time-history analysis are significantly influenced by the ground motions input. In order to reduce record-to-record variability and obtain a more accurate estimate of structural responses, a few methods for selection and scaling of ground motions have been developed [2, 4, 8–17]. The nonlinear time-history analysis is routinely adopted for the seismic design of base-isolated buildings, and some more advanced methods have been proposed, such as the weighted scaling methods [18–20] or the selection of standard records and synthetic accelerograms scaled by the PGV [21]. Among these methods, more attention has been given to amplitude linear scaling for a real record and its response spectral matching with the target spectrum [8–13, 15, 18–24].

In the ground motion scaling and spectral matching procedure, the spectral compatibility between the record's response spectrum and the target spectrum is mainly verified by the sum of the squared error (SSE) [8, 11, 18–20] or the general root mean square error [9, 10, 15, 24]. Error indexes should be minimized so that the record can realize the optimal spectral matching. Either the arithmetic values or the logarithm values of response spectra were adopted to calculate the error indexes in several different published studies. Arithmetic values were used in references [8–10, 13–15, 18–20, 24] since engineers are more familiar with arithmetic mean and design spectra in seismic codes can be taken directly as target spectra as well. Meanwhile, some researchers [11, 12, 22, 23] used the logarithm values of response spectra because logarithmic values are consistent with the assumption that the structural seismic responses are log-normally distributed. Logarithmic values are commonly used in the probabilistic seismic hazard analysis (PSHA) research field. The target spectra derived from the PSHA of a given site, such as the uniform spectrum (UHS) [25, 26] and the conditional mean spectrum (CMS) [11], were also fit for using the logarithm values. Until now, there have been no serious investigations regarding the effects of coordinate values on the scaling of the ground motions. It has not been ascertained whether the scale factors (SFs) for a record are the same under the two coordinates systems. Furthermore, for the same target spectra, it has not been ascertained if the spectral matching procedure is performed using the arithmetic values and logarithmic values and whether the structural EDPs predicted by the two procedures are similar.

In this paper, the 3-, 9-, and 20-story steel moment resisting frame structures, which represent low-, medium-, and high-rise buildings, were taken as examples. Their seismic responses were evaluated by time-history analysis. The arithmetic values and logarithmic values of response spectra were both used in spectral matching with the target spectra and then the ground motions were selected and scaled for structural time-history analysis. The target spectra that matched with the NEHRP 1994 design spectra [27] were defined as the average spectral accelerations of the three ground motion sets. The three record sets were developed in the American SAC Steel Project and represent 50%, 10%, and 2% probabilities of being exceeded in 50 years. The EDPs predicted by the two coordinate systems were compared with each other and influence factors, such as the structural periods and nonlinear response degrees were also discussed.

2. Spectral Matching with Target Spectra

When the target spectrum is given, the sum of squared errors can be used to measure the compatibility between the spectrum of the selected ground motion and the target spectrum. When using arithmetic values, the error index, SSE_A, is calculated by the following equation [8]:

$$\mathrm{SSE}_A = \sum_{i=1}^{n}\left[\left(\mathrm{SF}\cdot S_a(T_i) - S_a^t(T_i)\right)^2\right], \tag{1}$$

where $S_a^t(T_i)$ and $S_a(T_i)$ are the target spectral acceleration and the record's (unscaled) spectral acceleration at period T_i, respectively, SF is the scale factor, n is the total number of discrete period points and should be greater than 50 over the entire range of the periods (i.e., $[T_m, 1.5T_1]$, T_1 is the first mode period of the structure) [11], and m is the number of vibration modes that can ensure that the cumulative modal mass participation ratio is greater than 90%, which considers the effects of the higher modes for the structural responses [13]. The upper bound is $2T_1$ according to ASCE 7-16 [6], indicating that the lowest useable frequency of the selected records has to be extremely low if the fundamental period of the structure is longer (e.g., $T_1 = 4.11$ s for the 20-story structure in this study). It will decrease the number of available records that can be used for selecting from the PEER NGA database. Hence, the upper bound is adopted as $1.5T_1$ in this study according to ASCE 7-10 [28].

To obtain a minimum SF for each record, the SSE_A between the record's scaled spectrum and the target spectrum are minimized using the least squares method; i.e., $\mathrm{dSSE}/\mathrm{dSF} \cong 0$, and the SF is determined by the following equation:

$$\mathrm{SF} = \frac{\sum_{i=1}^{n}\left[S_a^t(T_i)\cdot S_a(T_i)\right]}{\sum_{i=1}^{n}\left[\left(S_a(T_i)\right)^2\right]}. \tag{2}$$

When the logarithmic values are considered, the sum of squared errors (SSE_L) and the scale factors (SF) are determined by the following equations [11]:

$$\mathrm{SSE}_L = \sum_{i=1}^{n}\left[\ln\left(\mathrm{SF}\cdot S_a(T_i)\right) - \ln S_a^t(T_i)\right]^2, \tag{3}$$

$$\ln \mathrm{SF} = \frac{1}{n}\sum_{i=1}^{n}\left[\ln S_a^t(T_i) - \ln S_a(T_i)\right]. \tag{4}$$

In addition, 0.02 and 0.04 were both used as the intervals of the period under the arithmetic and logarithmic coordinates systems and the SFs calculated using the both period intervals are all the same. Thus, 0.02 was used as the interval of the period in this study. The dense interval can ensure that the SFs are not influenced by the chosen coordinates systems.

In this paper, the spectral matching methods that use arithmetic values and logarithmic values of response spectra are referred to as the ASM and LSM method, respectively.

3. Definition of the Target Spectrum

Somerville [29] put forward three sets of ground motions in the SAC project that were selected based on the probabilistic seismic hazard analysis (PSHA) and matched with the NEHRP 1994 design response spectra [27]. These records represented 50/50, 10/50, and 2/50 seismic hazard levels in Los Angeles (i.e., 50%, 10%, and 2% probabilities of being exceeded in 50 years at the building site). Each set consisted of 20 records (i.e., 10 ground motions each with two orthogonal components). For simplicity, the three

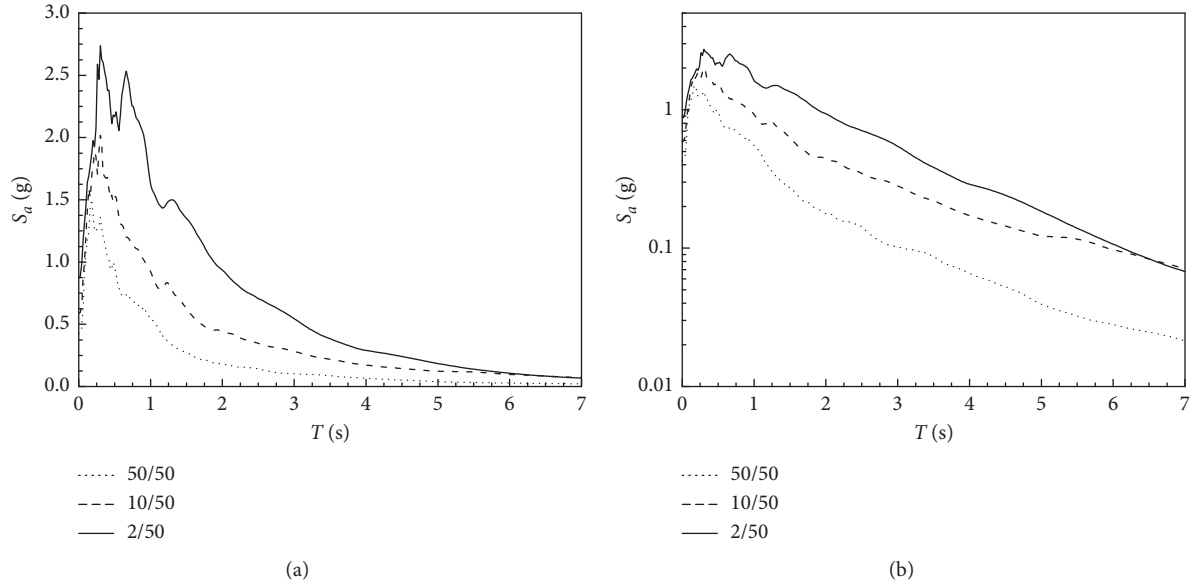

Figure 1: Target spectra plotted on (a) arithmetic and (b) logarithmic scales, 50/50, 10/50, and 2/50 sets ($\xi = 2\%$).

probabilities of exceedance or seismic hazard levels are all denoted as 50/50, 10/50, and 2/50 in the figures and tables in this work. Most of these records are real earthquake records, but there are several simulated ground motions in the record set of the 2/50 hazard level. The average (arithmetic mean) spectrum of each set of records is defined as the target spectrum representing the given hazard level. The target spectra representing the three hazard levels with a damping ratio of $\xi = 2\%$ are plotted in Figure 1 on the arithmetic scale (Figure 1(a)) and logarithmic scale (Figure 1(b)). The damping ratio is consistent with that of the three steel structures used as analysis models.

4. The Referenced Structures for Analysis

The 3-, 9-, and 20-story steel moment resisting frame structures used as analysis models in this work were initially designed for the SAC Phase II Steel Project [30], assuming that they would be located in Los Angeles. The buildings were not actually constructed, but they represent typical short-, medium-, and high-rise buildings in regions where there is a high risk of earthquakes. Therefore, these buildings were adopted to investigate the effects of the ASM and LSM methods on the results generated by nonlinear structural time-history analysis. More detailed information is provided in references [30, 31].

The finite element models (FEMs) of the buildings were built based on the platform of ABAQUS 6.12 [32] according to the structural details in reference [30]. The moment resisting frames are located at the perimeter of the structure. This design practice resulted in the presence of many interior frames which were designed to suffer from gravity loads only. There is no need to build the interior frames in analysis models. Only the moment resisting frames which resistant the horizontal forces, such as wind loads and earthquake loads, were modeled as two-dimensional frames that represented half of the structure in one direction [30]. B22 elements were used to model the beams and columns. It was assumed that plastic hinges were present only at the end of all structural beams and at the end of the columns at the first floor. The bilinear material constitutive model with the strain-hardening ratio of 0.01 was applied to the steel material. Rayleigh damping with a damping ratio of 2% was used for the first and second vibration modes. The Finite Element Modeling (FEM) took into account the effect of the P-Delta and the shear behavior of the Panel Zone according to reference [31].

Table 1 lists the lower three or four vibration periods and the modal-mass participation factors for the three structures. For the 3-, 9-, and 20-story structures, the lower two, four, and three modes should be considered in the selection and scaling of ground motions, respectively.

5. Selection and Scaling of Ground Motions

5.1. Ground Motions for Selection. We only used real records for selection and scaling in this study. Based on preliminary selection criteria [33],including the earthquake magnitude ($M_W \geq 6$) and the fault rupture distance (20 km ~ 40 km), eligible real records were retrieved by the PEER-NAG Database. The records came from six earthquake events and were comprised of 40 components taken from the 20 stations with two orthogonal components (see Table 2). The near-fault ground motions were not included in these records.

5.2. Scale Factors of Ground Motions. For the 3-, 9-, and 20-story structures at the three seismic hazard levels, the relative errors of SFs for the 40 record components are shown in Figure 2, which were calculated by the ASM method using equation (2) and by the LSM method using equation (4). The relative errors are defined as the differences between the SFs calculated by the LSM method and by the ASM method

Table 1: Vibration periods of the 3-, 9-, and 20-story structures.

Model	Vibration mode	Periods (s)	Modal mass participation ratio	Cumulative modal mass participation ratio
3-story	1st	1.00	0.828	0.828
	2nd	0.31	0.135	0.963
	3rd	0.16	—	—
9-story	1st	2.15	0.731	0.731
	2nd	0.81	0.109	0.840
	3rd	0.45	0.044	0.884
	4th	0.29	0.019	0.903
20-story	1st	4.11	0.755	0.755
	2nd	1.47	0.115	0.870
	3rd	0.86	0.038	0.908

Table 2: 20 stations with two-component ground motions.

ID number	Comp.	Event	Station	M_w	dR_{up} (km)	PGA (g)	PGV (cm/s)	PGD (cm)
1	AND270	Loma Prieta (89/10/18)	1652 Anderson Dam	7.0	21.40	0.24	20.3	7.7
2	AND360					0.24	18.4	6.7
3	BLD090	Northridge (94/01/17)	24157 LA-Baldwin Hills	6.7	31.30	0.24	14.9	6.2
4	BLD360					0.17	17.6	4.8
5	CCN090	Northridge (94/01/17)	24389 LA-Century City	6.7	25.75	0.26	21.1	6.7
6	CCN360					0.22	25.2	5.7
7	CLW-LN	Landers (92/06/28)	23 Coolwater	7.3	21.20	0.28	25.6	13.7
8	CLW-TR					0.42	42.3	13.8
9	TCU047-N	ChiChi (99/09/20)	Tcu047	7.6	33.01	0.41	40.2	22.2
10	TCU047-W					0.30	41.6	51.1
11	TCU095-N	ChiChi (99/09/20)	Tcu095	7.6	43.44	0.71	49.1	24.5
12	TCU095-W					0.38	62.0	51.8
13	WST000	Northridge (94/01/17)	90021LA-N Westmoreland	6.7	29.00	0.40	20.9	2.3
14	WST270					0.36	20.9	4.3
15	TCU045-N	ChiChi (99/09/20)	Tcu045	7.6	24.06	0.50	39.0	14.3
16	TCU045-W					0.47	36.7	50.7
17	I-ELC180	Imperial Valley (40/05/19)	117 El Centro array #9	6.9	8.30	0.31	29.8	13.3
18	I-ELC270					0.21	30.2	23.9
19	TAF021	Kern County (52/07/21)	1095 Taft Lincoln School	7.7	41.00	0.16	15.3	9.2
20	TAF111					0.18	17.5	9.0
21	CHY036-N	ChiChi (99/09/20)	CHY036	7.6	20.38	0.21	41.4	34.2
22	CHY036-W					0.29	38.9	21.2
23	FAR000	Northridge (94/01/17)	90016 LA –N faring Rd	6.7	23.90	0.27	15.8	3.3
24	FAR090					0.24	29.8	4.7
25	GLP177	Northridge (94/01/17)	90063 Glendale, Las Palmas	6.7	25.40	0.36	12.3	1.9
26	GLP267					0.21	7.4	1.7
27	HCH090	Loma Prieta (89/10/18)	1028 Hollister City Hall	7.0	28.20	0.25	38.5	17.8
28	HCH180					0.22	45.0	26.1
29	H-CHI012	Imperial Valley (79/10/15)	6621 Chihuahua	6.5	28.70	0.27	24.9	9.1
30	H-CHI282					0.25	30.1	12.9
31	STN020	Northridge (94/01/17)	90091 LA, Saturn St	6.7	30.00	0.47	34.6	6.5
32	STN110					0.44	39.0	6.4
33	SVL270	Loma Prieta (89/10/18)	1695 Sunnyvale, Colton Ave.	7.0	28.80	0.21	37.3	19.1
34	SVL360					0.21	36.0	16.9
35	TCU042-N	ChiChi (99/09/20	TCU042	7.6	23.34	0.20	39.3	23.9
36	TCU042-W					0.24	44.8	46.9
37	TCU107-N	ChiChi (99/09/20)	TCU107	7.6	20.35	0.16	47.4	32.8
38	TCU107-W					0.12	36.8	39.8
39	YER270	Landers (92/06/28)	22074 Yermo Fire Station	7.3	24.90	0.25	51.5	43.8
40	YER360					0.15	29.7	24.7

divided by the SFs calculated by the ASM method. For the 3-story structure, nearly all of the relative errors are positive. For the 9- and 20-story structures, the negative relative errors appear at the 50/50 seismic hazard level; however, more than half of the record components have positive relative errors. In general, for most of the record

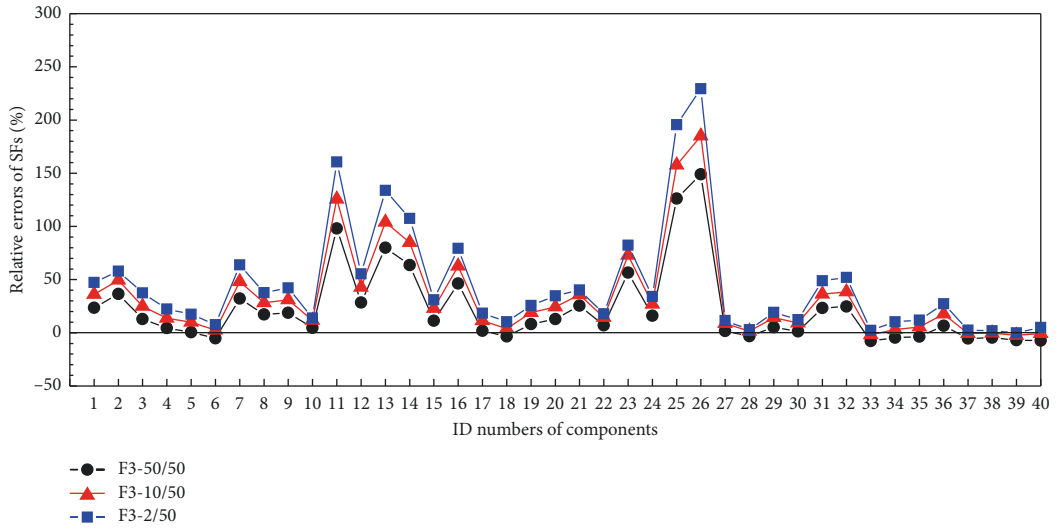

(a)

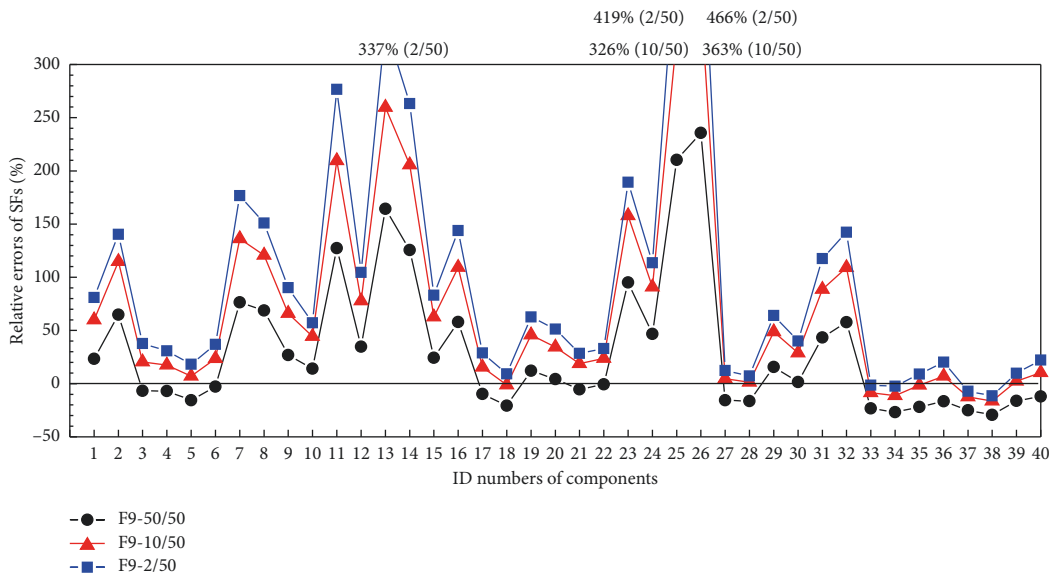

(b)

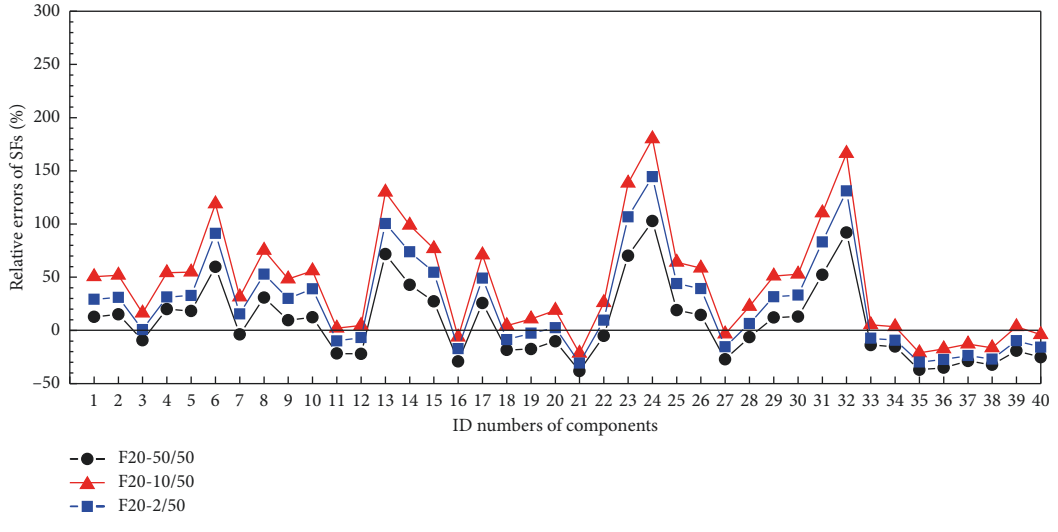

(c)

FIGURE 2: . Comparison of the relative errors of SFs between the ASM and LSM methods: (a) 3-story structure, (b) 9-story structure, and (c) 20-story structure.

components, the SFs calculated by the LSM method are significantly larger than those calculated by the ASM method, and the relative errors are as high as 50% to 200%. Additionally, except for the 2/50 set for the 20-story structure, the relative errors of the SFs increase as the seismic hazard levels increase.

Figure 2 also shows that the relative errors of SFs for the 9-story structure are larger than those of the other two buildings. It should be noted that the larger values (absolute values) in the response spectra would contribute more to the error index SSE_A (SSE_L) than the lower values in the response spectra, when SSE_A and SSE_L are calculated using equations (1) and (3), respectively.

If both the target spectrum and the response spectrum of a record use arithmetic values, the value of the SSE_A will mostly depend on the spectral values in the acceleration and velocity sensitive regions (corresponding to the short and medium-short periods, respectively) in the response spectrum; the SFs of the record will also be influenced. The degree of influence on SFs depends on the period range for spectral matching, which is determined by the structural periods.

While logarithmic values were used in the spectral matching procedure, the values of the SSE_L and SFs mostly depend on the different period ranges from the ASM method. Because the values of the target spectral acceleration and the record's spectral acceleration will both tend to zero at the very long periods, then their logarithmic values will go toward minus infinity. Because logarithmic functions have monotonicity, the spectral values in the displacement sensitive region (corresponding to long and very long periods) in the response spectrum will contribute more to the values of SF. The character of the LSM will benefit the seismic analysis of more flexible structures (e.g., high-rise buildings and long-span bridges) that have long first-mode periods.

For example, for the component I-ELC180 of the 9-story structure at the 2/50 hazard level, Figure 3(a) shows the relationship between the arithmetic values of the target spectral acceleration and the scaled record's spectral acceleration (i.e., "S_a^t" and "$\mathrm{SF} \times S_a$"); their corresponding logarithm values (i.e., "ln S_a^t" and "ln $(\mathrm{SF} \times S_a)$") are illustrated in Figure 3(b). The main control period ranges, in which the SSE_A (SSE_L) mostly depend on the spectral values, are presented in Figures 3(a) and 3(b). For clarity, the absolute values of "ln S_a^t" and "ln $(\mathrm{SF} \times S_a)$" are illustrated by the dash lines (see Figure 3(b)). The period matching range ([0.29 s, 3.23 s]) determined by the fundamental period of the 9-story structure ($T_1 = 2.15$ s) is shown in Figures 3(a) and 3(b).

5.3. Selection of Ground Motions. The number of records required for dynamic analyses has a significant effect on estimating the mean structural responses. Bommer and Acevedo [1] suggested that seven records might be adequate to produce an acceptable low dispersion of the structural response, while other researchers suggested that 10 records were required at least to obtain a stable mean of the structural dynamic responses. However, Reyes and Kalkan [12] considered that seven records were sufficient because the estimation accuracy of inelastic deformations of the SDOF system did not significantly increase when the number of records increased to 10. Current seismic design codes generally recommend seven (e.g., Eurocode 8 [5] and IBC-2012 [34]) or eleven (ASCE 7-16 [6]) as the required number of records. It should be mentioned that the minimum number of records required for dynamic analyses is affected by many situations, such as the purpose (i.e., the estimated mean or distribution of the structural response), the accuracy of predicted structural responses, the probability of structural collapse, and the degree of structural nonlinearity [35]. If the statistical distribution of the structural responses or the probability of structural collapse is considered in the analysis, the required number of records would be more, i.e., 30 and 60 [22, 23, 36]. This study aims to investigate the structural mean response demands (e.g., interstory drift ratios) calculated by the ASM and LSM methods. Therefore, the adopted number of records is seven herein. Actually, 11 records are also used and the obtained structural response results are similar to that obtained with seven records.

Additionally, the SFs of the records should also be limited. Generally, SFs exceeding 6-7 (or even less) are not adopted for scaling records in time-history analysis. These heavily scaled motions have no longer anything to do with real earthquake episodes that induced strong ground motions [37, 38]. Therefore, the limitations of SFs in this study are four at the 50/50 and 10/50 hazard levels and six at the 2/50 hazard level.

The procedure for records selection by the ASM and LSM methods is summarized as follows: (1) only the components with SF less than 4.0 or 6.0 are selected; (2) the selected components are preliminarily ranked by the values of SSE_A (or SSE_L); (3) the optimal seven components with minimum SSE_A (or SSE_L) are finally selected for the structural time-history analysis. Moreover, in order to avoid the influence of the interdependency between the two-components recorded by the same station on structural responses, only one horizontal component of a station is selected.

Using the above procedure, seven components were selected for the three structures by the ASM and LSM methods, which are listed in Tables 3~5. For the 3- and 9-story structures at the same seismic hazard level, four to six components are selected simultaneously by the ASM and LSM methods. However, there are only two to four of these types of components for the 20-story structure. Therefore, the ranking results generated with the ASM and LSM methods are different, especially for longer-period structures (i.e., 20-story structure). The relative errors of the SFs for the components selected simultaneously by both methods are also listed in the rightmost column of Tables 3~5, and nearly all absolute values of their relative errors are less than 20%.

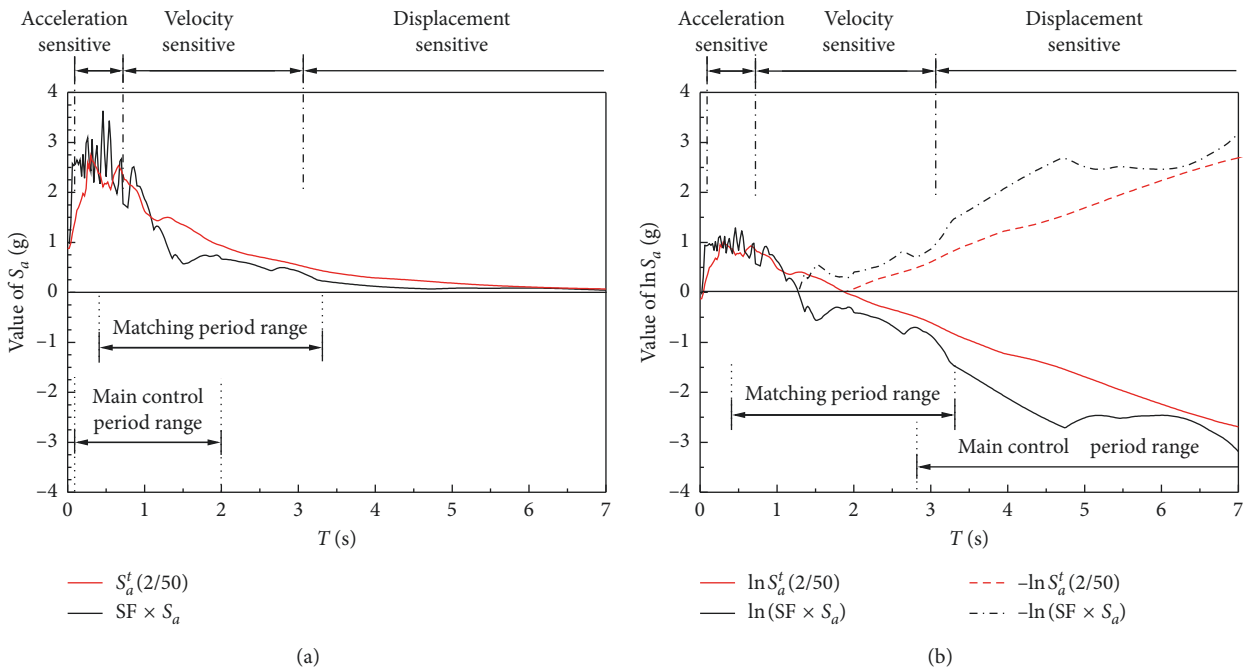

Figure 3: . Comparison of the (a) arithmetic and (b) logarithmic values of the target spectrum and the scaled record's spectrum (e.g., I-ELC180, 9-story, 2/50 hazard level).

Table 3: Components selected by ASM and LSM methods at the three hazard levels (3-story).

Hazard level	Sequence	ASM				LSM				
		ID number	Comp.	SF	SSE	ID number	Comp.	SF	SSE	Relative error (%)
50/50	1	36	TCU042-W	1.26	0.57	17	I-ELC180	1.037	1.256	2.0
	2	15	TCU045-N	0.94	0.64	20	TAF111	2.050	1.378	—
	3	17	I-ELC180	1.02	0.82	36	TCU042-W	1.341	1.440	6.5
	4	5	CCN090	1.40	0.85	5	CCN090	1.406	1.575	0.5
	5	3	BLD090	1.64	0.85	15	TCU045-N	1.044	1.840	11.4
	6	32	STN110	0.80	0.91	3	BLD090	1.854	1.981	12.8
	7	9	TCU047-N	0.91	0.92	32	STN110	1.003	2.222	24.8
10/50	1	18	I-ELC270	2.26	1.54	18	I-ELC270	2.34	1.03	3.9
	2	35	TCU042-N	2.42	1.72	35	TCU042-N	2.55	1.10	5.4
	3	34	SVL360	2.56	2.13	5	CCN090	2.52	1.10	10.0
	4	5	CCN090	2.29	2.26	34	SVL360	2.63	2.03	3.0
	5	15	TCU045-N	1.52	2.31	3	BLD090	3.32	2.08	—
	6	40	YER360	2.52	2.61	20	TAF111	3.67	2.18	—
	7	4	BLD360	3.12	2.89	29	H-CHI012	2.11	2.26	—
2/50	1	30	H-CHI282	3.01	6.01	30	H-CHI282	3.38	1.82	12.3
	2	18	I-ELC270	3.80	6.21	39	YER270	3.13	1.98	0.0
	3	6	CCN360	3.75	6.97	38	TCU107-W	3.84	2.46	2.0
	4	39	YER270	3.13	7.04	27	HCH090	3.44	2.74	11.6
	5	38	TCU107-W	3.77	9.26	22	CHY036-W	2.74	3.44	—
	6	15	TCU045-N	2.55	9.33	10	TCU047-W	2.55	4.52	—
	7	27	HCH090	3.09	9.90	8	CLW-TR	2.39	4.57	—

6. Structural Response Analysis

6.1. Structural Benchmark Demands. In code-based seismic design checks as well as performance-based engineering assessments, the structural responses of interstory drift ratios are often taken as the EDPs. It is commonly assumed that EDPs are log-normally distributed [39]; therefore, the median value and the geometric mean of EDPs are consistent and many researchers used the median to represent structural seismic demands [11, 12, 22, 23]. However, some seismic design codes (e.g., Eurocode 8 and ASCE 7-16) use the average value (arithmetic mean) of EDPs if at least seven ground motions are required for time-history analysis. Therefore, the "true" structural responses—i.e., "benchmark seismic demands"—are defined as both the arithmetic mean and median (geometric mean) of the EDPs under the

Table 4: Components selected by ASM and LSM methods at the three hazard levels (9-story).

Hazard level	Sequence	ID number	ASM			LSM				
			Comp.	SF	SSE	ID number	Comp.	SF	SSE	Relative error (%)
50/50	1	15	TCU045-N	0.95	0.36	17	I-ELC180	0.90	1.69	−9.7
	2	17	I-ELC180	1.00	0.45	19	TAF021	2.06	1.74	12.1
	3	36	TCU042-W	1.19	0.46	30	H-CHI282	1.06	1.78	—
	4	3	BLD090	1.60	0.49	6	CCN360	1.28	1.93	—
	5	9	TCU047-N	0.92	0.50	9	TCU047-N	1.16	2.22	26.9
	6	32	STN110	0.82	0.55	15	TCU045-N	1.18	2.37	24.3
	7	19	TAF021	1.84	0.58	31	STN020	1.46	2.74	—
10/50	1	18	I-ELC270	2.20	1.04	18	I-ELC270	2.17	1.51	−1.3
	2	35	TCU042-N	2.35	1.07	3	BLD090	3.25	1.54	20.5
	3	5	CCN090	2.23	1.38	35	TCU042-N	2.32	1.77	−1.4
	4	40	YER360	2.54	1.48	5	CCN090	2.39	2.01	7.0
	5	3	BLD090	2.70	1.71	40	YER360	2.80	2.43	10.3
	6	15	TCU045-N	1.58	1.94	27	HCH090	1.83	2.85	—
	7	20	TAF111	2.98	1.98	30	H-CHI282	2.30	2.90	—
2/50	1	18	I-ELC270	3.83	3.96	5	CCN090	4.60	1.76	18.3
	2	35	TCU042-N	4.11	4.02	18	I-ELC270	4.18	1.79	9.1
	3	39	YER270	3.16	4.59	35	TCU042-N	4.48	1.95	9.0
	4	5	CCN090	3.89	4.98	39	YER270	3.47	2.09	9.8
	5	30	H-CHI282	3.17	5.50	28	HCH180	2.73	2.22	—
	6	27	HCH090	3.15	5.59	30	H-CHI282	4.44	3.41	40.0
	7	22	CHY036-W	2.36	7.29	21	CHY036-N	3.46	4.06	—

Table 5: Components selected by ASM and LSM methods at the three hazard levels (20-story).

Hazard level	Sequence	ID number	ASM			LSM				
			Comp.	SF	SSE	ID number	Comp.	SF	SSE	Relative error (%)
50/50	1	17	I-ELC180	0.90	0.11	9	TCU047-N	1.21	3.42	—
	2	30	H-CHI282	0.93	0.12	30	H-CHI282	1.05	4.84	12.8
	3	6	CCN360	1.08	0.13	28	HCH180	0.54	5.08	—
	4	31	STN020	1.35	0.14	23	FAR000	3.75	6.32	—
	5	19	TAF021	1.89	0.16	2	AND360	2.25	6.69	—
	6	27	HCH090	0.75	0.19	20	TAF111	1.54	7.38	—
	7	15	TCU045-N	0.98	0.19	15	TCU045-N	1.24	9.01	27.2
10/50	1	28	HCH180	1.17	0.52	18	I-ELC270	2.22	4.02	4.5
	2	3	BLD090	3.32	0.69	28	HCH180	1.44	4.44	22.6
	3	18	I-ELC270	2.13	0.70	9	TCU047-N	3.22	4.71	—
	4	5	CCN090	2.24	0.82	38	TCU107-W	1.16	8.00	—
	5	16	TCU045-W	2.77	0.88	39	YER270	1.50	8.22	—
	6	40	YER360	2.22	0.88	29	H-CHI012	3.39	8.24	—
	7	11	TCU095-N	2.61	1.00	15	TCU045-N	3.30	9.58	—
2/50	1	5	CCN090	4.45	1.80	30	H-CHI282	4.74	5.78	33.2
	2	28	HCH180	2.30	2.06	28	HCH180	2.45	5.88	6.5
	3	18	I-ELC270	4.16	3.21	9	TCU047-N	5.49	6.02	—
	4	39	YER270	2.82	4.24	5	CCN090	5.91	9.19	32.7
	5	30	H-CHI282	3.56	4.65	18	I-ELC270	3.79	9.70	−8.8
	6	16	TCU045-W	5.34	5.37	15	TCU045-N	5.63	14.07	—
	7	38	TCU107-W	2.70	5.58	22	CHY036-W	2.54	15.15	—

earthquake excitations of the 50/50, 10/50, and 2/50 sets of ground motions proposed by the SAC project (shown in Figure 4). Since the arithmetic mean of interstory drift ratios is a little larger than the geometric mean for all three structures at the three seismic hazard levels, it will not significantly affect the conclusions of the structural response analysis.

Pushover analysis is conducted to confirm the degree of the structural nonlinear response. As shown in Figure 5, the three structures are in a nonlinear stage when the roof drift ratios increase to 0.07 and must be in a nonlinear stage at the 10/50 and 2/50 hazard levels.

6.2. Structural Response Analysis. The relative errors are defined as the difference between the mean (median) of the structural responses due to the selected seven records and their corresponding benchmark demands divided by the

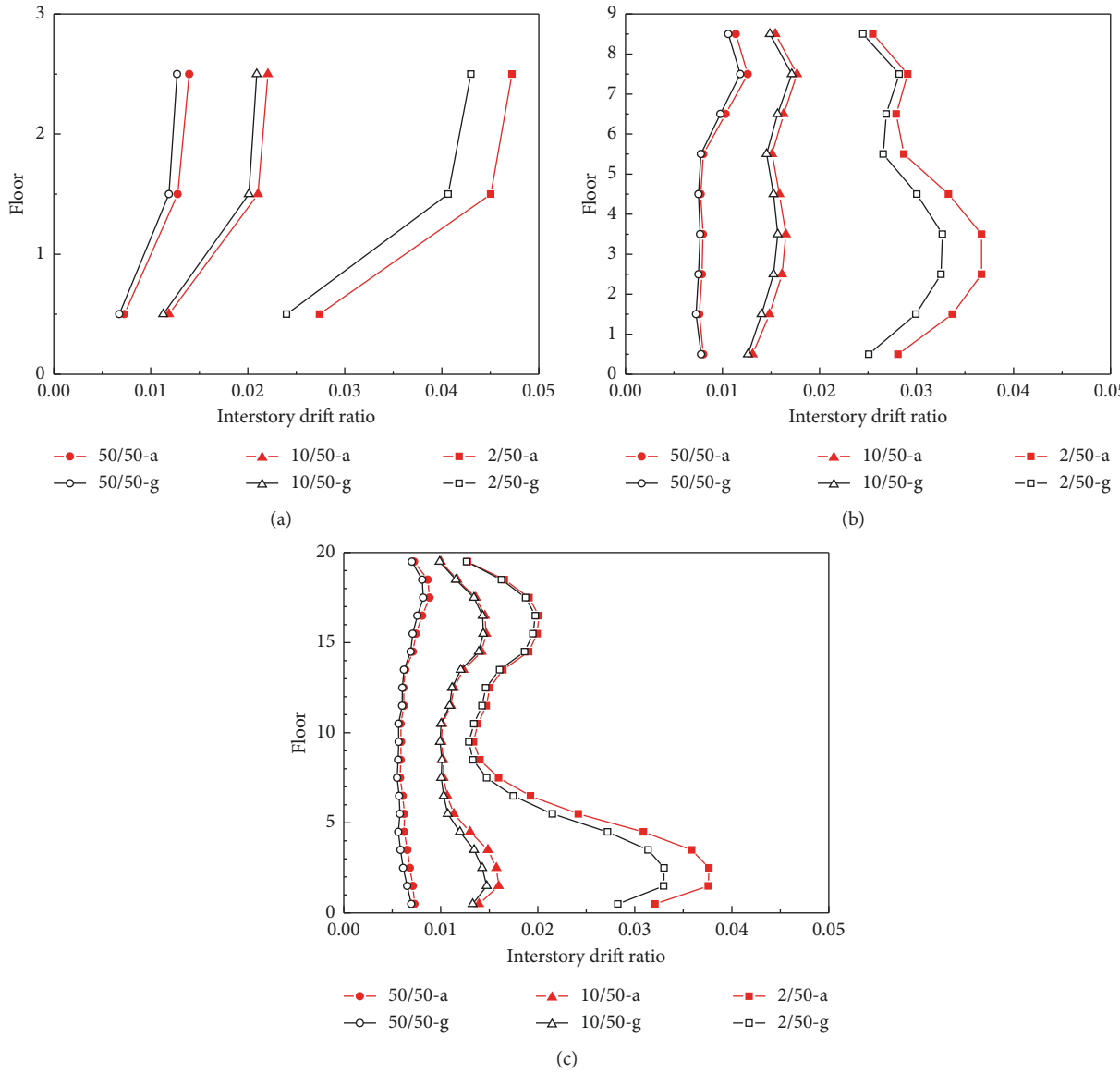

FIGURE 4: Arithmetic mean and geometric mean of interstory drift ratios for the (a) 3-, (b) 9-, and (c) 20-story structures at 50/50, 10/50, and 2/50 seismic hazard levels ("a" represents arithmetic mean and "g" represents logarithmic mean).

benchmark demands. The relative errors of the peak interstory drift ratio (PIDR) demands over the heights of the three structures based on benchmark mean and median demands using the ASM and LSM methods at the three hazard levels are plotted in Figure 6.

According to either the mean or median of benchmark structural responses, the LSM method generally has a somewhat larger relative error (algebraic value) than the ASM method, if the same structures at the same seismic hazard are considered. Therefore, the LSM method may generate more "conservative" estimates of the structural response as compared to the ASM method. This result is consistent with the trend of the SFs which is that the SFs by the LSM method are usually larger than that by the ASM method. It is important to point out that nearly all of the relative errors of all groups are within the range of ±20%. In other words, both the LSM and ASM methods can be used to predict the mean or median of structural responses. In addition, the component TCU045-W is excluded from the statistical analysis because it could induce a very large displacement response of the 20-story structure at the 2/50 seismic hazard level by the ASM method (Figures 6(e) and 6(f)).

The coefficient of variation (COV), defined as the ratio between the sample standard deviation and the sample mean or median, was used to assess the effectiveness of the ASM and LSM methods to reduce dispersion in the PIDR demands. Figure 7 shows the COVs of the PIDR demands over the height of the three structures calculated by both the LSM and ASM methods at the three hazard levels. For the benchmark mean and median demands, the COVs are very similar for the same structure and at the same hazard level.

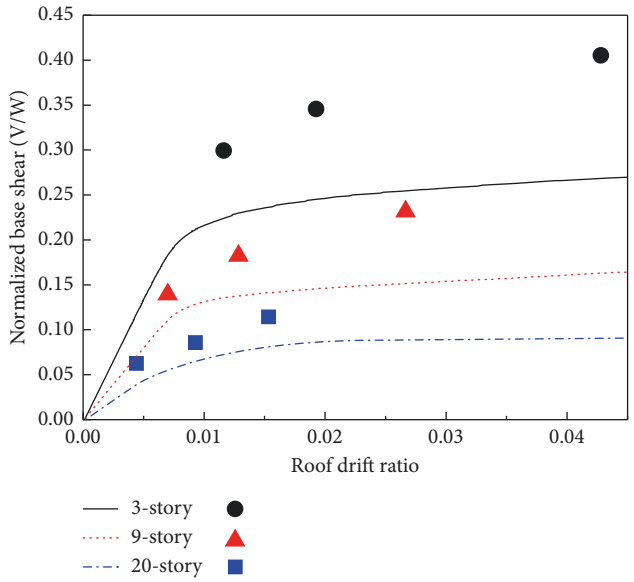

Figure 5: Global pushover curves for the 3-, 9-, and 20-story structures (scatter points with the same shape from left to right represent the benchmark mean demands at 50/50, 10/50, and 2/50 seismic hazard levels).

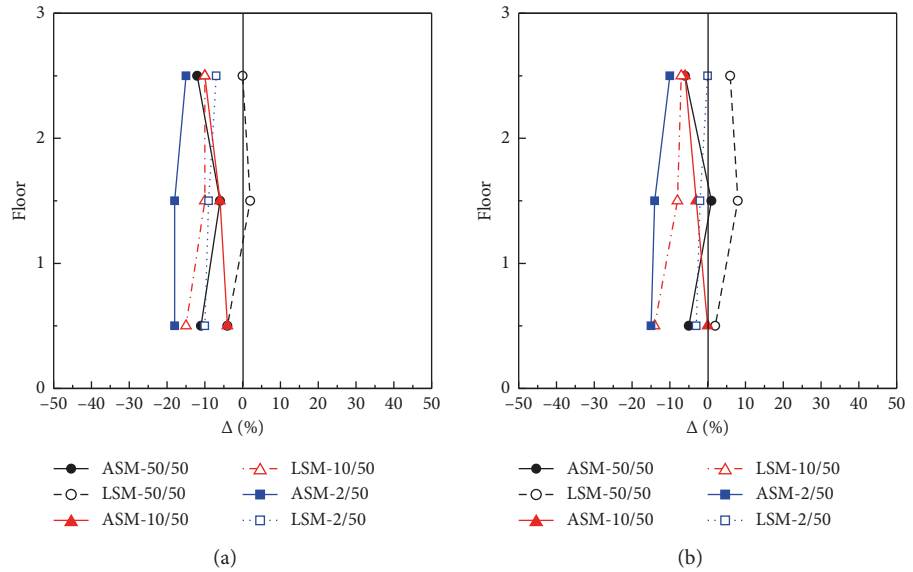

Figure 6: Continued.

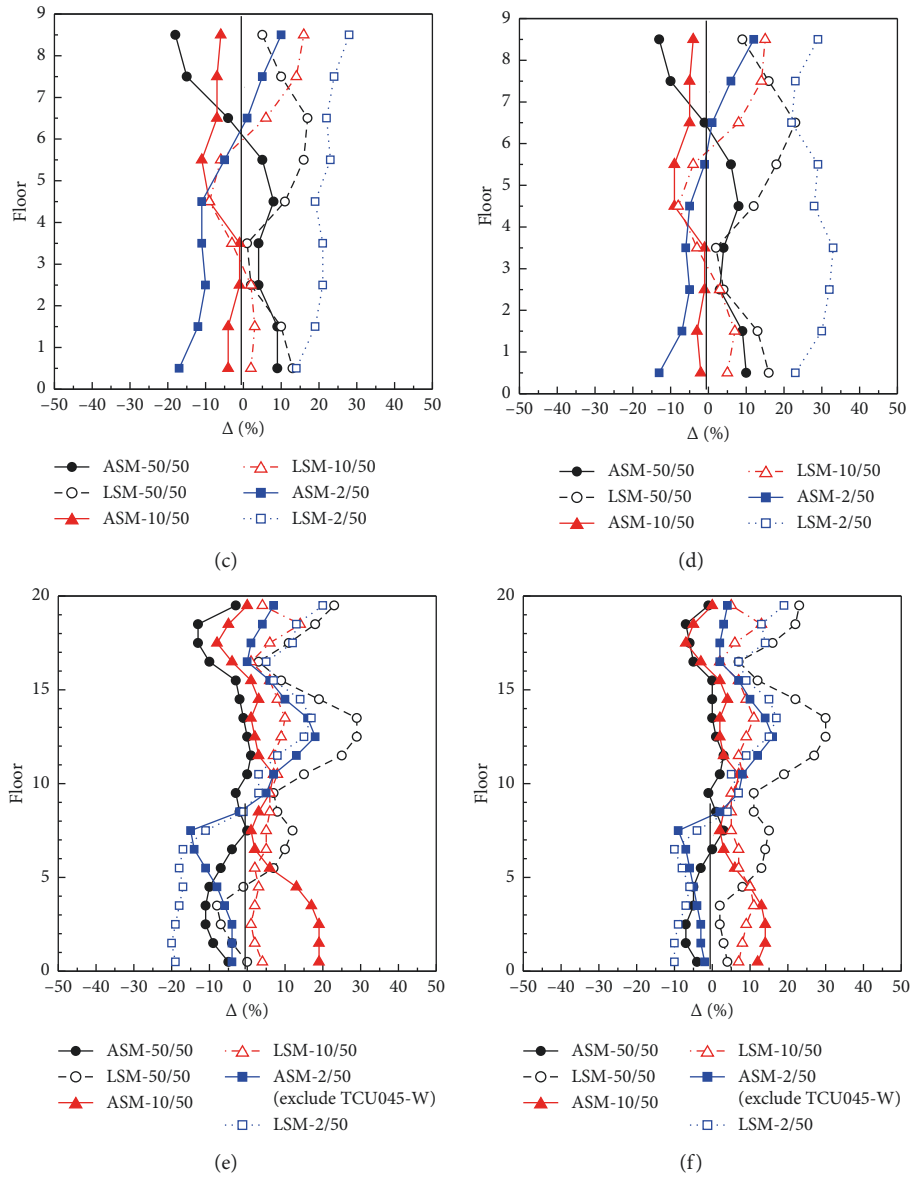

FIGURE 6: Relative errors of PIDR demands over the height of the 3-, 9-, and 20- structures at the 50/50, 10/50, and 2/50 hazard levels by both ASM and LSM methods based on benchmark mean and median demands: (a) 3-story, mean, (b) 3-story, median, (c) 9-story, mean, (d) 9-story, median, (e) 20-story, mean, and (f) 20-story, median.

For long-period structures (i.e., 9-story and 20-story structures), the LSM method has lower COVs compared to the ASM method at all three hazard levels. This trend is even more pronounced for the 20-story structure with a more severe nonlinear response, and the COVs at the weakest floor of the 20-story structure by the LSM method are only 30% of that by the ASM method at the 2/50 hazard level. Moreover, if we only compare the COVs by the LSM method, the values of COV are very similar at all three hazard levels. Therefore, the structural nonlinear responses have little effect on the above trend as well as on the values of COV when using the LSM method. However, the COVs using the ASM method are significantly affected by the structural responses, and the values are larger for a more severe nonlinear response. Therefore, for longer-period structures, such as the 9- and 20-story buildings analyzed in this work, using logarithmic values of response spectra is more applicable for spectral matching than using arithmetic values.

The COVs of the 3-story structure are a little different with that of the 9- and 20-story structures, and the COVs are dependent on the structural responses. While the 2/50 ground motion set was used as input and the 3-story structure suffered the most severe nonlinear responses (shown in Figure 5), the COVs for the ASM method are larger than that of the LSM method. In contrast, the COVs by the ASM method are smaller than those of the LSM method, when the structure is subjected to the excitations of the other two ground motion sets selected at the 50/50 and 10/50 hazard levels.

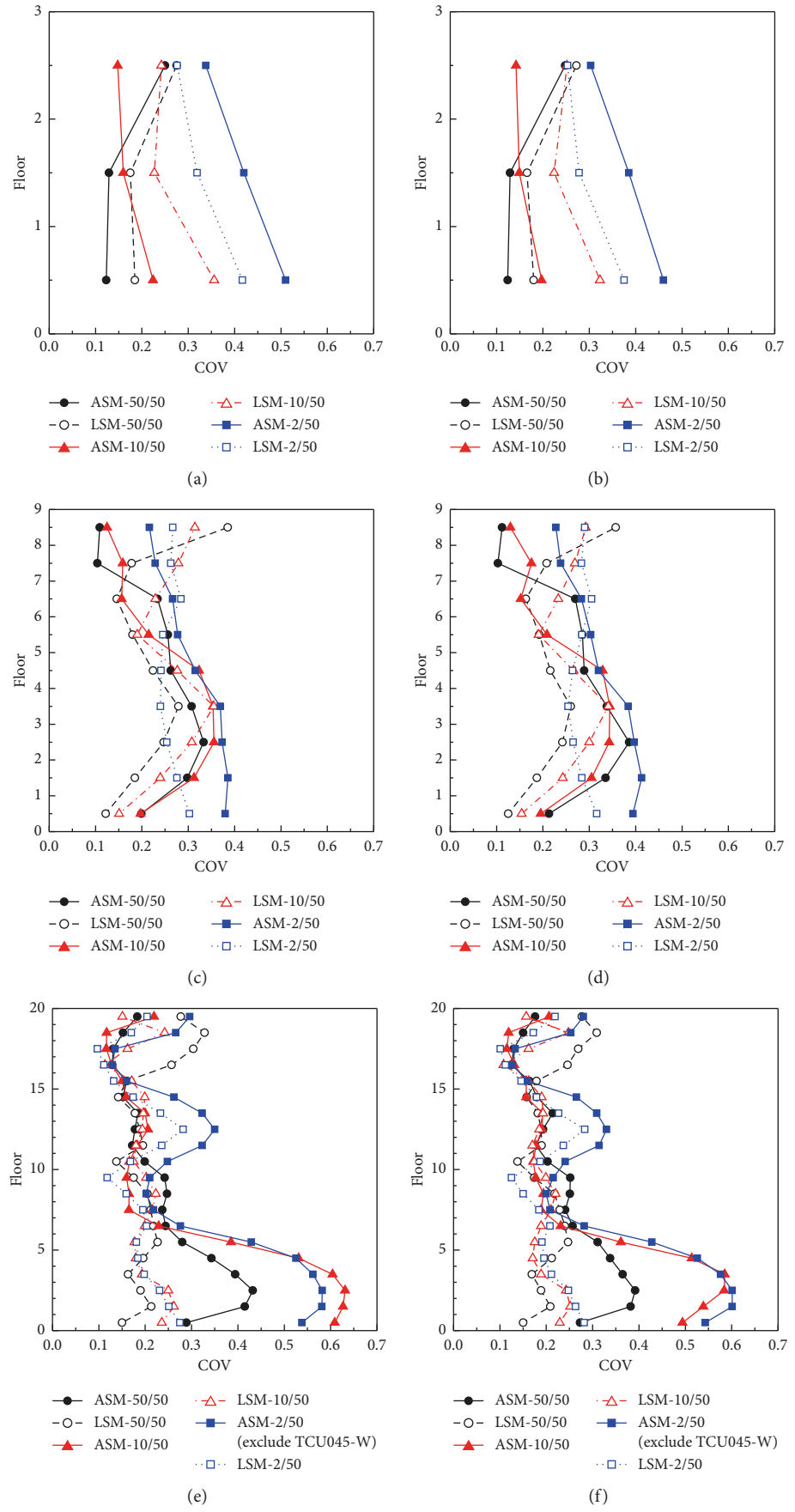

Figure 7: COVs of PIDR demands over the height of the 3-, 9-, and 20- structures at the 50/50, 10/50, and 2/50 hazard levels by both ASM and LSM methods: (a) 3-story, mean, (b) 3-story, median, (c) 9-story, mean, (d) 9-story, median, (e) 20-story, mean, and (f) 20-story, median.

7. Conclusions

The least square method is generally used to verify the compatibility between the spectrum of the selected ground motion and the target spectrum and to calculate the scale factors of the selected records. However, until now, there have not been any serious investigations performed regarding the effects of the coordinate values on the scaling of ground motions. This study aimed to investigate the influence of using arithmetic and logarithmic values in a spectral matching procedure (i.e., the ASM and LSM method) on the results of nonlinear structural time-history analysis. The 3-, 9-, and 20-story steel moment resisting frame structures, which represent low-, medium-, and high-rise buildings in the Los Angeles area in the SAC Steel Project, were used as examples. Based on the records that were selected and scaled by the ASM and LSM methods, the structural dynamic responses were compared at the three seismic hazard levels (i.e., 50%, 10%, and 2% probabilities exceeded in 50 years). The main conclusions are summarized below:

(1) The SFs by the LSM method are significantly larger than those derived from the ASM method for low-, medium-, and high-rise buildings (i.e., 3-, 9-, and 20-story structures) at the three seismic hazard levels. This is mainly because the values of the SSE_A for the ASM method mostly depends on the spectral values in the acceleration and velocity sensitive regions. Nevertheless, the values of the SSE_L for the LSM method mostly depends on the spectral values in the displacement sensitive region. The trends will affect the values of SF. This indicates that the ASM method may be more suitable for short-period structures and the LSM method is more suitable for long-period structures. Meanwhile, the ranking and selection of the records are also different. There are only approximately four (for 3- and 9-story structures) or two (for 20-story structure) components simultaneously selected by both methods among the optimal seven components selected for nonlinear structural time-history analysis.

(2) The relative errors of the PIDR demands can all be controlled within an acceptable range (±20%) by both methods, when the demands obtained by both methods are compared with the benchmark mean (or median) demands. Thus, the LSM and ASM methods both can be used to predict the mean or median of structural responses. However, the relative errors (algebraic value) calculated by the LSM method are larger than that of the AMS method; thus, the structural mean (or median) responses predicted by the LSM method will be slightly larger.

(3) For long-period structures (i.e., 9-story and 20-story structures), the LSM method performed better at reducing variability in the structural responses results as compared to the ASM method. This advantage is more significant for longer-period structures (e.g., 20-story structure) with more severe nonlinear responses (e.g., 2/50 seismic hazard level).

Data Availability

Data used in this study can be found in the Pacific Earthquake Engineering Research Center Strong Motion Database at ngawest2.berkeley.edu (last accessed January 2019). All data, models, or code generated or used in this study are available from the corresponding author upon request.

Conflicts of Interest

The authors declare that there are no conflicts of interest regarding the publication of this paper.

Acknowledgments

This research was supported by the National Natural Science Foundation of China (Grant no. 1778206).

References

[1] J. J. Bommer and A. Acevedo, "The use of real earthquake accelerograms as input to dynamic analysis," *Journal of Earthquake Engineering*, vol. 8, no. 1, pp. 43–91, 2004.

[2] PEER GMSM Working Group, "Evaluation of ground motion selection and modification methods: predicting median interstory drift response of buildings," PEER Rep., PEER, Berkeley, CA, USA, 2009.

[3] E. I. Katsanos, A. G. Sextos, and G. D. Manolis, "Selection of earthquake ground motion records: a state-of-the-art review from a structural engineering perspective," *Soil Dynamics and Earthquake Engineering*, vol. 30, no. 4, pp. 157–169, 2010.

[4] J. W. Baker and C. Lee, "An improved algorithm for selecting ground motions to match a conditional spectrum," *Journal of Earthquake Engineering*, vol. 22, no. 4, pp. 708–723, 2018.

[5] CEN, EN 1998-3, *Eurocode 8: Design of Structures for Earthquake Resistance*, European Committee for Standardization, Brussels, Belgium, 2005.

[6] ASCE/SEI 7-16, *Minimum Design Loads and Associated Criteria for Buildings and Other Structures*, American Society of Civil Engineers, Reston, VA, USA, 2016.

[7] E. Miranda and H. Aslani, "Probabilistic response assessment for building specific loss estimation," Technical Report, Pacific Earthquake Engineering Research Center PEER, Berkeley, CA, USA, 2003.

[8] E. Kalkan and A. K. Chopra, "Practical guidelines to select and scale earthquake records for nonlinear response history analysis of structures," Technical Report, Earthquake Engineering Research Institute, Berkeley, CA, USA, 2010.

[9] K. Beyer and J. J. Bommer, "Selection and scaling of real accelerograms for bi-directional loading: a review of current practice and code provisions," *Journal of Earthquake Engineering*, vol. 11, no. sup1, pp. 13–45, 2007.

[10] I. Iervolino, C. Galasso, and E. Cosenza, "REXEL: computer aided record selection for code-based seismic structural analysis," *Bulletin of Earthquake Engineering*, vol. 8, no. 2, pp. 339–362, 2010.

[11] J. W. Baker, "Conditional mean spectrum: tool for ground-motion selection," *Journal of Structural Engineering*, vol. 137, no. 3, pp. 322–331, 2011.

[12] J. C. Reyes and E. Kalkan, "Required number of records for ASCE/SEI 7 ground motion scaling procedure," Open-File Report, U.S. Geological Survey, Reston, VA, USA, 2011.

[13] E. I. Katsanos and A. G. Sextos, "Structure-specific selection of earthquake ground motions for the reliable design and assessment of structures," *Bulletin of Earthquake Engineering*, vol. 16, no. 2, pp. 583–611, 2018.

[14] S. Marasco and G. P. Cimellaro, "A new energy-based ground motion selection and modification method limiting the dynamic response dispersion and preserving the median demand," *Bulletin of Earthquake Engineering*, vol. 16, no. 2, pp. 516–681, 2018.

[15] P. E. Mergos and A. G. Sextos, "Selection of earthquake ground motions for multiple objectives using genetic algorithms," *Engineering Structures*, vol. 187, pp. 414–427, 2019.

[16] L. Moschen, R. A. Medina, and C. Adam, "A ground motion record selection approach based on multiobjective optimization," *Journal of Earthquake Engineering*, vol. 23, no. 4, pp. 669–687, 2019.

[17] A.-A. I. Theophilou, "A ground motion selection and modification method through stratified sampling," *Bulletin of Earthquake Engineering*, vol. 17, no. 2, pp. 637–655, 2019.

[18] Y. N. Huang, *Performance assessment of conventional and base-isolated nuclear power plants for earthquake and blast loadings*, Ph.D. dissertation, University at Buffalo, State University of New York, Buffalo, NY, USA, 2008.

[19] G. Ozdemir and M. C. Constantinou, "Evaluation of equivalent lateral force procedure in estimating seismic isolator displacements," *Soil Dynamics and Earthquake Engineering*, vol. 30, no. 10, pp. 1036–1042, 2010.

[20] D. R. Pant and M. Maharjan, "On selection and scaling of ground motions for analysis of seismically isolated structures," *Earthquake Engineering and Engineering Vibration*, vol. 15, no. 4, pp. 633–648, 2016.

[21] P. Pan, D. Zamfirescu, M. Nakashima et al., "Base-isolation design practice in Japan: introduction to the post-Kobe approach," *Journal of Earthquake Engineering*, vol. 9, no. 1, pp. 147–171, 2005.

[22] G. Wang, "A ground motion selection and modification method capturing response spectrum characteristics and variability of scenario earthquakes," *Soil Dynamics and Earthquake Engineering*, vol. 31, no. 4, pp. 611–625, 2011.

[23] W. Du, C. L. Ning, and G. Wang, "The effect of amplitude scaling limits on conditional spectrum-based ground motion selection," *Earthquake Engineering & Structural Dynamics*, vol. 48, no. 9, pp. 1030–1044, 2019.

[24] L. Lombardi, F. De Luca, and J. Macdonald, "Design of buildings through linear time-history analysis optimising ground motion selection: a case study for RC-MRFs," *Engineering Structures*, vol. 192, pp. 279–295, 2019.

[25] C. A. Cornell, "Probabilistic analysis of damage to structures under seismic loads," in *Dynamic Waves in Civil Engineering*, D. A. Howells, I. P. Haigh, and C. Taylor, Eds., pp. 473–488, Wiley, New York, NY, USA, 1971.

[26] R. K. McGuire, *Seismic Hazard and Risk Analysis*, Vol. 221, Earthquake Engineering Research Institute, Oakland, CA, USA, 2004.

[27] FEMA, 1997, *NEHRP Guidelines for the Seismic Rehabilitation of Buildings*, Standard FEMA 273, Federal Emergency Management Agency, Washington DC, USA, 1997.

[28] ASCE/SEI 7-10, *Minimum Design Loads and Associated Criteria for Buildings and Other Structures*, ASCE Standard no.007-10, American Society of Civil Engineers, Reston, VA, USA, 2010.

[29] P. Somerville, *Development of Ground Motion Time Histories for Phase 2 of the FEMA/SAC Steel Project*, SAC Joint Venture, Sacramento, CA, USA, 1997.

[30] Y. Ohtori, R. E. Christenson, B. F. Spencer, and S. J. Dyke, "Benchmark control problems for seismically excited nonlinear buildings," *Journal of Engineering Mechanics*, vol. 130, no. 40, pp. 366–385, 2004.

[31] A. Gupta and H. Krawinkler, *Seismic Demands for Performance Evaluation of Steel Moment Resisting Frame Structures (SAC Task 5.4.3)*, Palo Alto, U.S. Blume Earthquake Engineering Center, Stanford University, Stanford, CA, USA, 1999.

[32] Abaqus, Online Documentation 6.12, Dassault Systems, 2012.

[33] E. Miranda and J. Ruiz-García, "Evaluation of approximate methods to estimate maximum inelastic displacement demands," *Earthquake Engineering & Structural Dynamics*, vol. 31, no. 3, pp. 539–560, 2002.

[34] IBC, 2012, *International Building Code*, International Code Council, Washington DC, USA, 2012.

[35] J. Hancock and J. J. Bommer, "A state of knowledge review of the influence of strong motion duration on structural damage," *Earthquake Spectra*, vol. 22, no. 3, pp. 827–845, 2006.

[36] A. Catalán, A. Benavent-Climent, and X. Cahís, "Selection and scaling of earthquake records in assessment of structures in low-to-moderate seismicity zones," *Soil Dynamics and Earthquake Engineering*, vol. 30, no. 1-2, pp. 40–49, 2010.

[37] P. K. Malhotra, "Strong-motion records for site-specific analysis," *Earthquake Spectra*, vol. 19, no. 3, pp. 557–578, 2003.

[38] J. Watson-Lamprey and N. Abrahamson, "Selection of ground motion time series and limits on scaling," *Soil Dynamics and Earthquake Engineering*, vol. 26, no. 5, pp. 477–482, 2006.

[39] C. A. Cornell, F. Jalayer, R. O. Hamburger, and D. A. Foutch, "Probabilistic basis for 2000 SAC federal emergency management agency steel moment frame guidelines," *Journal of Structural Engineering*, vol. 128, no. 4, pp. 526–533, 2002.